Neuron, Vol. 23, 385–397, June, 1999, Copyright ©1999 by Cell Press

Efficacy of Thalamocortical and Intracortical Synaptic Connections: Quanta, Innervation, and Reliability

Ziv Gil,* Barry W. Connors,†‡ and Yael Amitai*
*Department of Physiology
Zlotowski Center for Neuroscience
Faculty of Health Sciences
Ben-Gurion University
Beer-Sheva 84105
Israel
†Department of Neuroscience
Division of Biology and Medicine
Brown University
Providence, Rhode Island 02912

Summary

Thalamocortical (TC) synapses carry information into the neocortex, but they are far outnumbered by excitatory intracortical (IC) synapses. We measured the synaptic properties that determine the efficacy of TC and IC axons converging onto spiny neurons of layer 4 in the mouse somatosensory cortex. Quantal events from TC and IC synapses were indistinguishable. However, TC axons had, on average, about 3 times more release sites than IC axons, and the mean release probability at TC synapses was about 1.5 times higher than that at IC synapses. Differences of innervation ratio and release probability make the average TC connection several times more effective than the average IC connection, and may allow small numbers of TC axons to dominate the activity of cortical layer 4 cells during sensory inflow.

Introduction

The neocortex receives sensory information from the thalamus. Only about 5%–20% of the excitatory synapses onto layer 4 neurons in the cortex are thalamocortical (TC) (White and Keller, 1989; Peters and Payne, 1993). Most of the rest are intracortical (IC), originating mainly from neurons of the same layer and layer 6 (McGuire et al., 1984; Ahmed et al., 1994). The sensory responses of cortical neurons are determined by the strength and patterns of input from TC and IC synapses and by local inhibitory circuits. The relative importance of each input to the construction of receptive field properties in primary sensory areas of cortex is unclear. This issue has been intensively investigated for orientation selectivity in visual cortex. Some studies have concluded that spatially aligned TC inputs alone account for orientation selectivity, while others suggest that recurrent IC circuits provide essential enhancement of weak TC inputs (for discussions, see Hubel and Wiesel, 1962; Douglas et al., 1995; Reid and Alonso, 1995, 1996; Somers et al., 1995; Ferster et al., 1996; Chung and Ferster, 1998). The cellular mechanisms that generate visual receptive fields are likely to be of general importance for understanding sensory processing. However, almost nothing is known about the basic synaptic properties that determine the relative efficacy of TC and IC connections in any sensory system. Sensory processing in the neocortex cannot be understood without characterizing the specific physiology of its various types of synapses (Chance et al., 1998).

Using in vitro methods, we recently found that TC and IC synapses have very different dynamics and sensitivities to neuromodulators (Gil et al., 1997), but more basic questions remain. Central synapses vary widely in their strength and reliability (Korn and Faber, 1991; Murthy et al., 1997; Walmsley et al., 1998). What is the efficacy of the synaptic connection between a thalamic relay neuron and a cortical neuron, or between two cortical neurons? Paired-cell or minimal-stimulation studies of various IC connections have shown a broad range of unitary excitatory postsynaptic potential (EPSP) amplitudes (e.g., Mason et al., 1991; Thomson et al., 1993; Volgushev et al., 1995; Stratford et al., 1996). Markram et al. (1997) suggested that synapses between cortical neurons of layer 5 possess a wide continuum of efficacies. The unitary properties of identified TC synapses have not been studied. However, a relatively strong and invariant connection has been inferred (Stratford et al., 1996), and extracellular cross-correlation studies in vivo suggest that TC connections are much stronger than IC connections in the visual system (Tanaka, 1983) and perhaps also in the somatosensory system (Johnson and Alloway, 1996).

We can define the mean efficacy of a synaptic connection between two neurons (E) as the amplitude of the unitary, single-axon response when activated at low frequency. E is then determined by three parameters, such that $E = q \cdot n \cdot p_r$, where q is the mean quantal size (i.e., the amplitude of the postsynaptic response to a single quantum of transmitter; Katz, 1969), n is the number of release sites contributed by the presynaptic axon to the postsynaptic cell, and p_r is the mean probability of transmitter release at each site. Here, we have used the TC slice preparation (Agmon and Connors, 1991) to study the relative efficacies of TC and IC connections onto layer 4 neurons. Our results imply that single-axon connections from thalamus to cortex are significantly more effective than IC connections; although quantal size is the same in the two tracts, TC connections have a higher innervation ratio and release probability than IC connections.

Results

Our basic strategy was to record from single spiny neurons of the primary somatosensory (barrel) cortex in vitro and independently measure the properties of TC and IC inputs to each cell (Gil and Amitai, 1996; Gil et al., 1997). The biocytin-stained cells we recovered (n =

‡To whom correspondence should be addressed (e-mail: barry_connors@brown.edu).

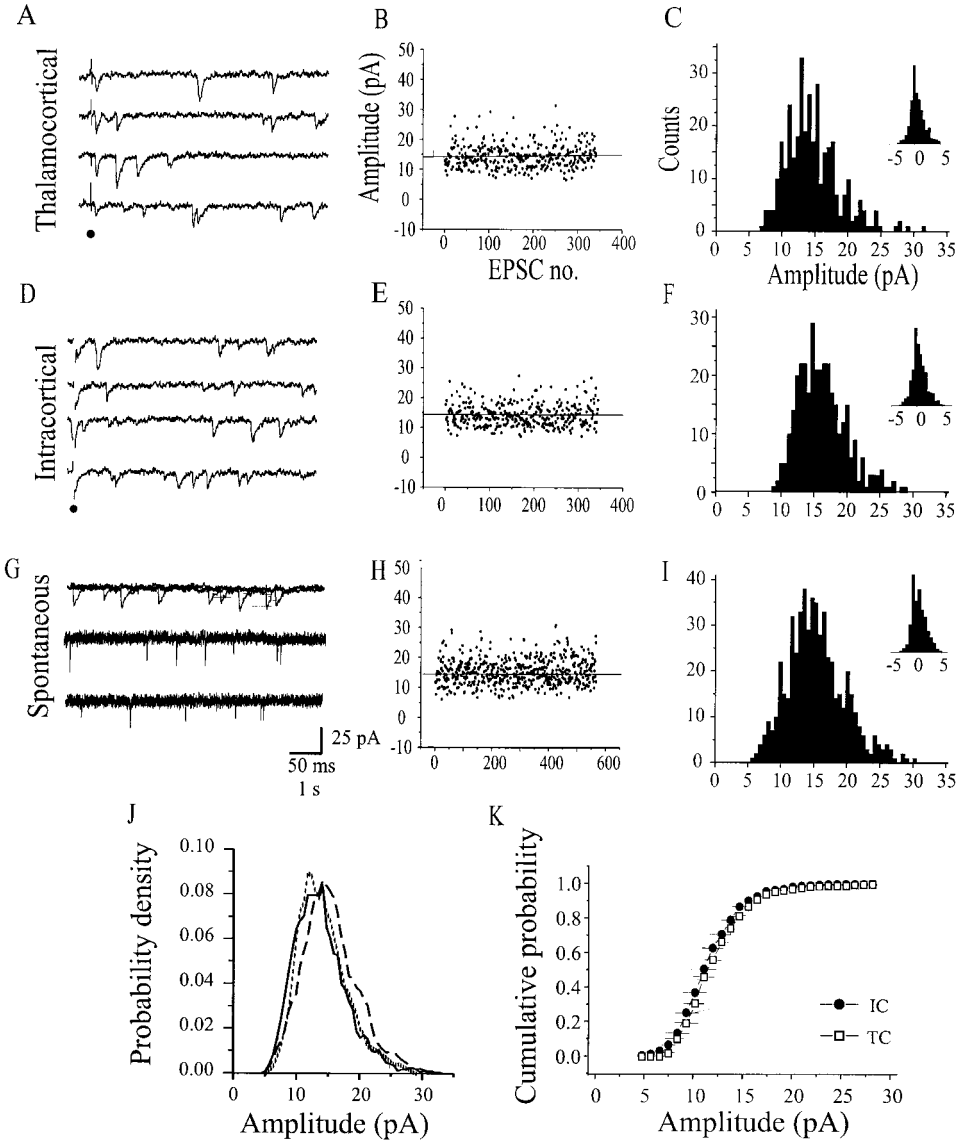

Figure 1. Asynchronous Release Reveals that Quantal TC and IC EPSCs Have Similar Amplitude Distributions

All data from (A) through (J) were derived from the same neuron.

(A and D) Examples of voltage clamp recordings of unitary EPSCs from a single cell, evoked by shocks to TC and IC axons, while bathed in Sr^{2+} solution. Dots mark times of stimuli.

(B and E) Asynchronous EPSC amplitudes as a function of occurrence sequence, illustrating stability of amplitudes for >300 events. Horizontal lines show the means.

(C and F) Amplitude histogram of the TC and IC asynchronous EPSCs. Histograms of background noise are displayed as insets.

(G) Spontaneous EPSCs in Sr^{2+}. Upper traces are four overlapped sweeps on the same time scale as (A) and (D). The lower two single traces have a slower time scale, showing the low frequency of spontaneous events.

(H and I) Stability plot and amplitude histogram of the spontaneous events.

(J) Probability density functions of the amplitudes of TC (dotted line), IC (solid line), and spontaneous (dashed line) EPSCs. The three functions show similar peaks and variances.

(K) Cumulative probability plot of asynchronous EPSCs evoked by TC (open squares) and IC (closed circles) pathways in all cells tested (n = 7), showing no statistical difference ($p > 0.3$). Data points and bars are mean ± SEM.

13) were small pyramidal cells or spiny stellate cells in layer 4 or on the border between layers 3 and 4. Unless otherwise noted, NMDA receptors were blocked and AMPA receptor–mediated excitatory postsynaptic currents (EPSCs) or EPSPs were recorded. As described in detail below (Figure 7), under control conditions the mean efficacy of single TC connections was significantly stronger than that of IC connections. The aim of our study was to determine the mechanisms for this difference in efficacy by estimating, in either absolute or relative terms, the quantal size, innervation ratio, and release probability for the TC and IC pathways.

Quantal Size of TC and IC Synapses (*q*)

The origins of spontaneous synaptic events in a cortical neuron are usually unknown. To measure the quantal size of TC and IC synapses selectively, it was necessary to evoke quantal events in such a way that their origin was identifiable. We used two different strategies: the induction of asynchronous release and the reduction of release probability.

Asynchronous Release in Sr^{2+}

When extracellular Sr^{2+} is substituted for Ca^{2+}, evoked transmitter release becomes asynchronous and prolonged, and single quantal events can be seen in isolation (Dodge et al., 1969; Abdul-Ghani et al., 1996; Oliet et al., 1996). In the presence of Sr^{2+}, a single stimulus to either TC or IC axons evoked a greatly increased frequency of small-amplitude synaptic currents that lasted for about 1 s (Figures 1A and 1D). We stimulated each pathway at <0.1 Hz and measured the amplitude distributions of isolated EPSCs during the 10–400 ms interval after each stimulus. The sizes of synaptic events were stable over the duration of the sampling period, as shown for a representative cell in Figures 1B and 1E, and they were well above the current noise (insets to Figures 1C, 1F, and 1I). The frequency of spontaneous EPSCs (about 0.5–1 Hz) was at least one order of magnitude lower than that of evoked synaptic events under the same conditions (Figure 1G). Thus, our samples of TC and IC EPSCs were contaminated $<10\%$ by spontaneous EPSCs. The amplitude distributions of TC and IC EPSCs within a single neuron were very similar to each other (Figures 1C and 1F) and to those of unidentified spontaneous EPSCs (Figures 1G–1I). Figure 1J shows the close similarity between the amplitude distributions of TC, IC, and spontaneous EPSCs for a single cell. Amplitude distributions were well fit by single Gaussians, apart from small tails at the large-amplitude end of the distributions. The Gaussian fits of pooled data from seven neurons yielded TC and IC EPSC amplitudes of 11.3 $\pm$ 1.4 pA and 11.5 $\pm$ 1.4 pA, respectively ($p > 0.3$). Figure 1K shows normalized cumulative probability distributions of EPSC amplitudes obtained from all neurons; there was no statistical difference between the TC and IC EPSCs. In addition, the time courses of TC and IC EPSCs were indistinguishable. Rise times were 1.8 $\pm$ 0.8 ms for IC and 1.8 $\pm$ 0.7 ms for TC; decay time constants were 26.1 $\pm$ 12.1 ms for IC and 27.9 $\pm$ 14.6 ms for TC (Figure 1). These kinetics are significantly slower than those of the AMPA receptor–mediated EPSCs recorded by Stern et al. (1992) in layer 4 cortical neurons, so our currents may have been filtered by the dendrites, the electronics, or both. Nevertheless, this filtering appeared to be similar for TC and IC synapses. Our data suggest that the mean sizes and shapes of quantal events from TC and IC synapses are identical.

To measure the unclamped quantal EPSP size, and to help rule out the possibility that voltage clamp errors selectively distorted the quantal size distribution of one of the pathways, we repeated the Sr^{2+} experiments under current clamp conditions (Figure 2). Again, there was no difference between the TC and IC pathways. The amplitude histograms (Figure 2B) and cumulative probability plots (Figure 2C) for EPSPs of both tracts were very similar ($n = 4$ neurons). The fits of Gaussian distributions to the TC and IC EPSP histograms implied quantal sizes of 0.38 $\pm$ 0.03 mV and 0.35 $\pm$ 0.03 mV, respectively ($p > 0.3$).

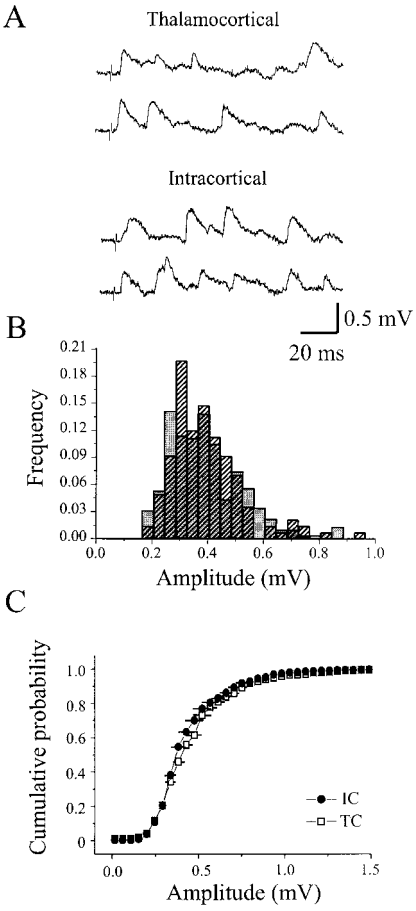

Figure 2. Asynchronous TC and IC EPSPs Display Similar Quantal Size Distributions in Sr^{2+} Solution

(A) Examples of current clamp recordings of asynchronous EPSPs evoked by TC (upper traces) and IC (lower traces) stimulation in a single cell. $V_m = -70$ mV.

(B) Amplitude histograms of TC-evoked (hatched bars) and IC-evoked (closed bars) EPSPs in the same cell as in (A), showing very similar distributions.

(C) Cumulative probability plot of TC (open squares) and IC (closed circles) EPSPs from four cells recorded as in (A), showing no difference between the two tracts ($p > 0.3$). Data points and bars are mean $\pm$ SEM.

Reduced Release Probability

To obtain an independent estimate of the size of single TC and IC quanta, we used extracellular Cd^{2+} to block the evoked entry of Ca^{2+} into presynaptic terminals. This reduces release probability, leads to frequent failures of synaptic transmission, and greatly increases the chances that successful transmission consists of minimally sized (presumed quantal) events. We added 10–20 μM Cd^{2+} to the perfusion solution and used low stimulus intensities (10–20 μA) to activate TC and IC axons. Under these conditions, more than 70% of stimuli failed to elicit a response, and EPSPs of successful stimuli were mostly quite small. Figures 3A–3C show examples of

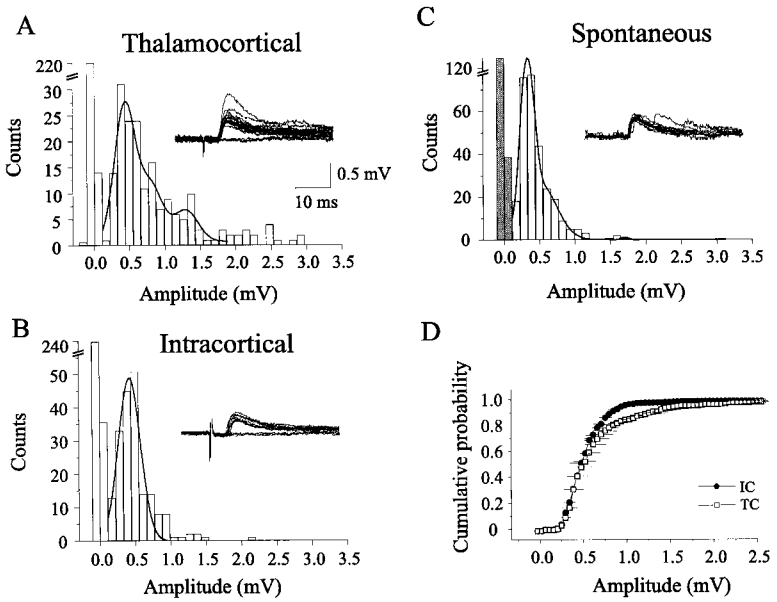

Figure 3. Low Release Probability Conditions Yield Similar Quantal EPSP Sizes in TC and IC Connections

Data were obtained from cells recorded in 10 μM Cd^{2+}-containing solution; (A) through (C) were obtained from a single neuron.

(A) Amplitude histogram of TC-evoked EPSPs; the line shows the sum of Gaussian functions fitted to the amplitude histogram. Example traces of successes and failures are displayed in the inset.

(B) Amplitude histogram of IC-evoked EPSPs.

(C) Amplitude histogram of spontaneous EPSPs. Note the similarly sized peaks of TC, IC, and spontaneous EPSPs. Gray bars are a measurement of baseline noise.

(D) Cumulative probability plot of TC (open squares) and IC (closed circles) EPSPs for all cells recorded in Cd^{2+} (n = 5). Data points and bars are mean ± SEM.

TC, IC, and spontaneous EPSPs from a single cell; their amplitude histograms all have prominent peaks between 0.3 and 0.6 mV, and except for the TC EPSPs there was a very low frequency of events larger than 1 mV. Fits of Gaussian functions to the amplitude distributions of five neurons yielded very similar mean sizes for the peak TC and IC EPSPs (0.37 ± 0.03 mV and 0.37 ± 0.04 mV, respectively; Figures 3A and 3B). The cumulative probability distributions were also very similar, except that the TC pathway had substantially more large events than the IC pathway (Figures 3A and 3D).

The results of the experiments in Cd^{2+} and Sr^{2+} were quantitatively very similar, supporting the conclusion that the main peaks of the EPSC/P amplitude distributions represent estimates of quantal size for the two sets of synapses. Furthermore, the amplitude distributions of TC and IC quanta were indistinguishable. The coefficient of variation (CV) of quantal EPSPs estimated with the two methods was relatively small and also similar between pathways: 0.26 and 0.23 for the TC and IC synapses, respectively. Large synaptic events (presumably derived from multiple quanta) were commonly observed only in the TC pathway, and only in the Cd^{2+} experiments.

Innervation Ratio of TC and IC Axons (*n*)

The presence of some large TC EPSPs evoked with Cd^{2+} in the bath, but not with Sr^{2+}, suggests two possibilities: (1) that TC axons have a higher innervation ratio than IC axons, i.e., each TC axon provides more release sites per postsynaptic neuron than each IC axon does; and (2) that the mean release probability of TC synapses is higher than that of IC synapses and remains relatively higher in the presence of the Cd^{2+}. These are not mutually exclusive. To examine the first possibility, we estimated the postsynaptic effect of activating single presynaptic TC or IC axons, under conditions of enhanced p_r in order to minimize p_r-dependent bias. When tested in control medium containing 2 mM Ca^{2+} and 2 mM Mg^{2+}, the paired-pulse ratio with a 50 ms interstimulus interval was 0.68 ± 0.02 for TC synapses and 0.95 ± 0.04 for IC synapses (see Gil et al., 1997). When the bath [Ca] was raised to 3 mM and [Mg] was lowered to 1 mM to increase p_r, the paired-pulse ratio was 0.50 ± 0.07 for TC and 0.52 ± 0.13 for IC synapses (n = 6). The reduced paired-pulse ratios imply that high [Ca]/[Mg] medium increases p_r in both pathways; the similarity between the TC and IC paired-pulse ratios further suggests that differences of p_r in the two pathways is insignificant under high [Ca]/[Mg] conditions.

Single axons of each pathway were activated using a "minimal-stimulation" protocol (Raastad et al., 1992; Stevens and Wang, 1995; Dobrunz and Stevens, 1997; Isaac et al., 1997). Stimulation intensity was minimized and adjusted to evoke all-or-none synaptic events that are presumed to originate from activation of a single presynaptic axon. Figure 4A illustrates an example of small, all-or-none EPSCs evoked by low-frequency TC stimulation in one neuron. Increasing the stimulus intensity gradually between 5.0 and 6.0 μA led to a reduction in the failure rate without a change in the amplitude of the EPSCs (Figure 4B). With stimulus intensity held at 5.8 μA, paired stimulus pulses (25 ms interval) resulted in consistent failures of either the first or the second EPSC, or both (data not shown; cf. Figures 4A and 5B). These results are consistent with the hypothesis that a single axon was being activated. The amplitude distribution histogram of EPSCs from this TC axon was notably narrow (CV = 0.07), was Gaussian in shape, had a single peak at 11 pA, and failed on 20% of the trials (Figure 4C). The mean amplitude is very similar to the quantal EPSC size estimated in the Sr^{2+} experiments. We conclude that this particular axon triggered a single release site on the recorded cortical cell. However, the small size and uniformity of minimal responses in this cell were not characteristic of TC axons; other neurons showed larger and more variable responses to TC stimulation. An example is shown in Figures 4D–4F, where minimal stimulus intensities elicited all-or-none responses, a failure rate greater than 60%, and yet amplitudes that varied between 8 and 190 pA.

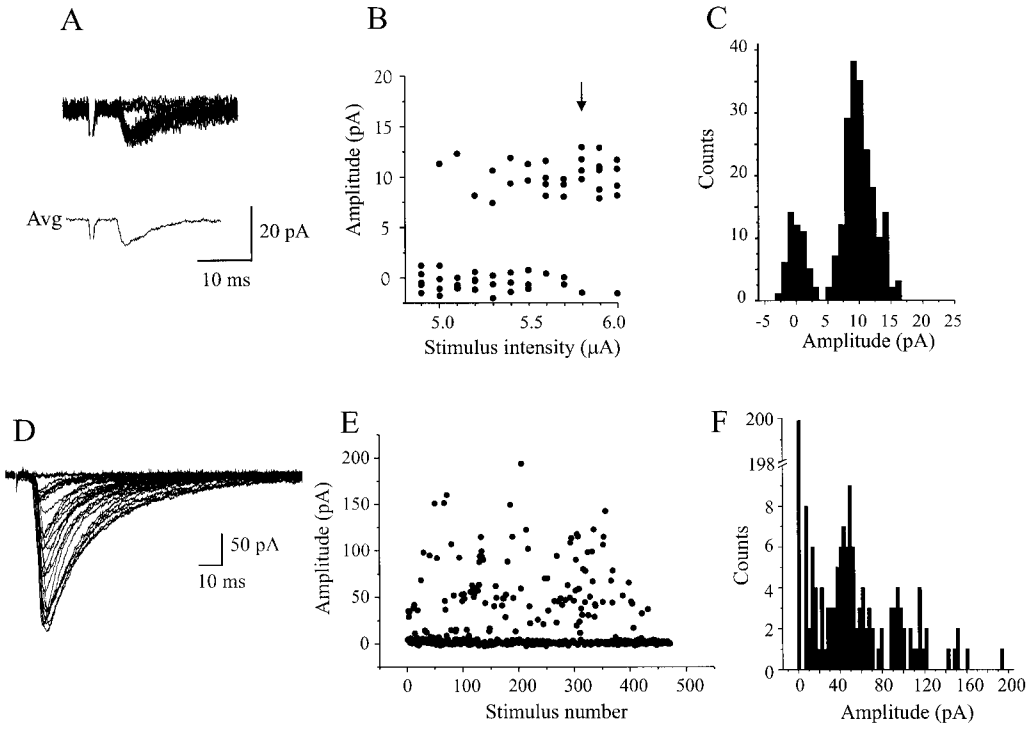

Figure 4. Minimal Stimulation of TC Axons Elicits EPSCs of Variable Amplitude

(A–C) Recordings from one neuron showing all-or-none EPSCs, apparently from a single TC release site.

(A) Example traces (upper) and the average of 50 successive events (lower).

(B) Gradually increasing stimulus intensity between 5.0 and 6.0 μA caused a reduction in failure rate without changing EPSC amplitudes. Arrow indicates the stimulus intensity used for collecting events for the amplitude histogram shown in (C).

(D–F) Data from another cell during minimal TC stimulation, showing examples of highly variable amplitudes (D), their stability over time (E), and their amplitude histogram (F). Stimulus intensity in this cell was adjusted to give >60% failures.

When the minimal-stimulation protocol was applied to evoke IC responses, the amplitude distributions tended to be smaller and less variable than those of TC responses (see examples in Figures 5B and 5C). As a measure of the EPSC amplitude variability generated by the minimal responses in each cell, we calculated the mean amplitude of the smallest and largest 5% of the sample distribution and the mean amplitudes (excluding failures) of the entire sample. Data from TC and IC inputs were compared. The smallest EPSCs from the two pathways were very similar to each other (9.1 ± 1.7 pA for TC axons, 9.4 ± 2.1 pA for IC axons, $p > 0.6$, $n = 11$ neurons; Figure 6A) and just slightly smaller than the mean quantal size estimated in the Sr^{2+} experiments. (We expect the smallest minimal EPSC sizes to be less than the Sr^{2+} estimate of quantal size, because the latter is the *mean* amplitude of the sample distribution, whereas the former is derived from the *smallest 5%* of responses in the sample.) The data are consistent with the hypothesis that the smallest of the minimal-stimulation EPSCs are generated by single quanta of transmitter derived from single release sites, and they reinforce the conclusion that TC and IC quanta are identical.

In contrast to the smallest minimal responses, there was a marked difference between the two pathways when the largest EPSCs were compared (Figure 6C). The largest EPSC evoked from the IC pathway was about 4 times the quantal size (48 pA), while the largest EPSC evoked by TC stimulation was 18 times the quantal size (190 pA; Figures 4D–4F). On average, the largest 5% of the TC EPSCs were significantly bigger than the largest IC-evoked EPSCs ($n = 11$ neurons, 77.4 ± 54.5 pA and 24.8 ± 8.8 pA for TC and IC, respectively; $p < 0.005$, t test; Figure 6C). The means of all sampled EPSC amplitudes from TC (28.8 ± 16.3 pA) and IC (16.2 ± 7.0 pA) pathways were also significantly different ($p = 0.02$, $n = 11$). The largest minimal-stimulation EPSCs for each axon in high [Ca] solution are a conservative estimate of the axon's maximal potency. If we divide the maximal potency by our estimate of quantal size (*q*, about 11 pA), we can approximate the number of release sites per axon (*n*). Accordingly, *n* is estimated to be 7.0 ± 4.9 for TC axons and 2.2 ± 0.8 for layer 4 IC axons.

To confirm that TC connections are stronger than IC connections under control ionic conditions, we repeated the minimal-stimulation experiments in solutions containing 2 mM [Ca] and 2 mM [Mg]. TC connections were indeed significantly stronger: excluding failures, the mean IC EPSC amplitude was 15.1 ± 2.5 pA ($n = 11$; Figure 7A), and the mean TC EPSC amplitude was 40.1 ± 7.6 pA ($n = 5$, $p < 0.001$; Figure 7B).

Relative Release Probability of TC and IC Synapses (p_r)

TC and IC synapses differ in their short-term dynamics—during repetitive stimulation, TC synapses depress

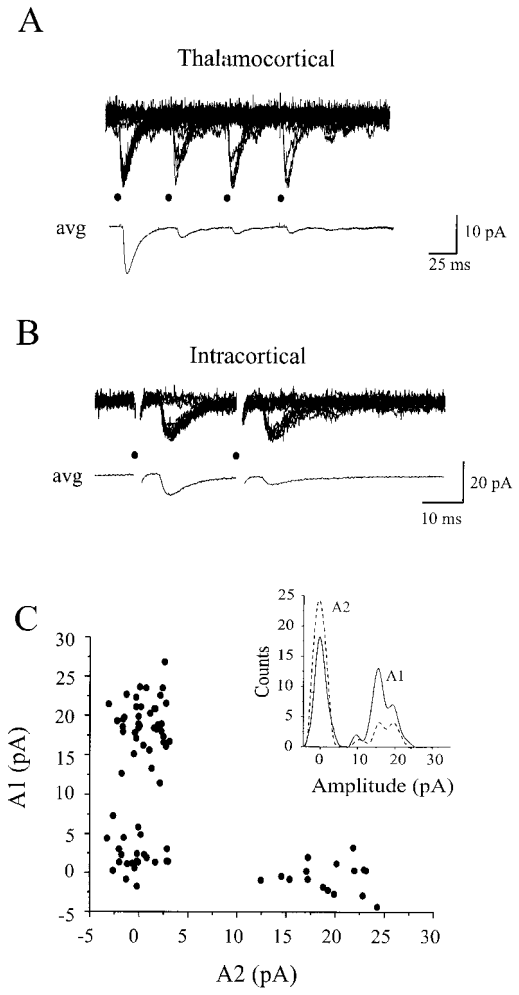

Figure 5. Short-Term Dynamics of Minimal TC and IC EPSCs

(A) All-or-none EPSCs evoked from a TC connection. Upper panel displays ten consecutive responses to a train of four stimuli at 20 Hz. Lower panel displays the average traces. Dots represent stimulation times.

(B) All-or-none EPSCs evoked by an IC axon. Upper panel displays eight consecutive responses to paired pulses at 50 Hz. Lower panel displays the average of the traces above.

(C) The amplitude of the first IC EPSC (A1) plotted against the amplitude of the second EPSC (A2); data are from the cell in (B). The inset displays amplitude histograms of A1 (continuous line) and A2 (dotted line). Although the peak amplitude of the first and second responses were very similar, the failure rate of A2 was significantly higher and depended on the success of A1.

strongly, while IC synapses tend either to depress moderately or to facilitate weakly (see above; see also Gil et al., 1997). Depression in both pathways was evident under conditions of minimal stimulation during trains of two to four shocks (at 20–50 Hz), and the results imply presynaptic involvement. Figures 5A and 5B illustrate data from connections with possible single-release sites (recorded under high [Ca]/[Mg] conditions); during trains to either the TC or the IC pathways, the failure rates of later stimuli were higher than those of the first stimulus, while the mean amplitude of successful EPSCs remained constant through the trains. For the TC axon in Figure 5A, the success rate was 0.87 at the first pulse and 0.22, 0.16, and 0.18 at the second, third, and fourth, respectively. The responses of another neuron during paired IC stimulation (25 ms interval) are shown in Figures 5B and 5C. The probability of evoking an EPSC with the first stimulus was 0.51, and when this occurred the second stimulus invariably failed. When the first stimulus failed, however, the second stimulus succeeded with a probability of 0.42. The amplitude distributions of the first and second responses were very similar (Figure 5C, inset). Only one TC connection and three IC connections had the characteristics of single-release sites, so more detailed comparisons between pathways and neurons were not possible. However, these results are consistent with the suggestion that synaptic depression in TC and IC pathways is due primarily to the decreased probability of transmitter release from presynaptic terminals (Gil et al., 1997).

Since short-term depression is stronger for TC synapses than IC synapses under control [Ca]/[Mg] conditions, and a presynaptic mechanism is implicated, it seemed likely that the average release probability (p_r) is higher at TC synapses than at IC synapses (Zucker, 1989; Debanne et al., 1996). To test this, we used an indirect method to compare the relative p_r of the two types of synapses in single neurons (Hessler et al., 1993; Rosenmund et al., 1993; Manabe and Nicoll, 1994): the rate of blockade of NMDA receptor–mediated EPSCs was measured during repetitive stimulation of TC and IC pathways in the presence of the NMDA antagonist MK-801. The method depends on the fact that NMDA channels must first be opened before they can be blocked by MK-801 and that the blockade is essentially irreversible during the time of an experiment. When synapses are activated at a constant frequency, the rate of NMDA channel blockade depends on the average probability of glutamate release. AMPA and $GABA_A$ receptors were blocked by DNQX (15 μM) and BMI (5 μM), respectively.

The basic properties of NMDA receptor–dependent EPSCs were evaluated for both the TC and IC pathways in each cell. Voltage dependence was similar for each, with negative slope conductance at holding potentials more negative than −20 mV and only very small currents below −40 mV (Figures 8A and 8B). Increasing the stimulus intensity resulted in larger amplitudes but did not change the voltage sensitivity of the EPSCs (data not shown). We did not observe any NMDA EPSCs with substantially less voltage dependence in either the IC or the TC pathway, as recently described for intra–layer 4 synapses within neocortex (Fleidervish et al., 1998).

The time courses of NMDA EPSCs in TC and IC pathways were indistinguishable (the decay time constants were 78 ± 30 ms for TC and 72 ± 25 ms for IC at +40 mV, 51 ± 14 ms for TC and 55 ± 13 ms for IC at −20 mV, mean ± SEM, n = 18 neurons). NMDA EPSC decay time constants varied more than 3-fold across neurons, and Figure 8C shows the strong correlation between values from TC and IC responses obtained from the same cells (r = 0.74, n = 17 neurons).

Holding potentials were subsequently kept at +40 mV and each pathway was stimulated alternately at 0.1 Hz. After establishing a stable baseline, stimulation was stopped, MK-801 (40 μM) was added to the bath, and stimulation was resumed 10 min later. NMDA EPSCs

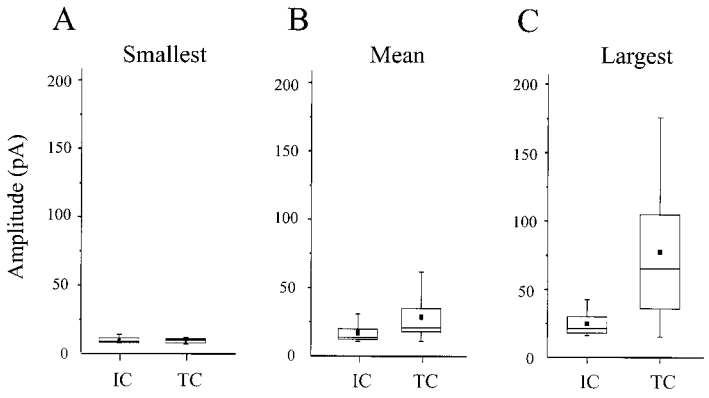

Figure 6. Summary of TC and IC Minimal Stimulation Results

Data are presented as box plots: the boxes delimit the 25th to 75th percentiles, the horizontal lines in the boxes plot the medians, the dots plot the average, and the vertical lines delimit the 5th to 95th percentiles ($n = 11$).

(A) The smallest evoked TC and IC EPSCs show similar amplitudes ($p > 0.6$). For each cell, the lowest 5% of the samples were averaged to obtain an estimate of "smallest EPSCs".

(B) The mean amplitudes of TC and IC EPSCs (excluding failures) are significantly different ($p = 0.02$).

(C) The largest TC EPSCs were significantly bigger than the largest IC EPSCs ($p < 0.01$). For each cell, the biggest 5% of the samples were averaged to obtain an estimate of "largest EPSCs".

from both pathways decayed progressively with repeated stimuli (Figure 9A). There were often residual EPSCs of up to 20% of control amplitude that were not blocked by MK-801 even after long periods of stimulation; residual EPSCs are commonly seen in MK-801 studies (e.g., Hessler et al., 1993; Manabe and Nicoll, 1994) and are blocked by APV (cf. Reid et al., 1997). Both TC and IC pathways were also tested with paired stimuli (25 ms interval) before MK-801 and after the 100th stimulus in the presence of the drug. In control conditions, TC connections were strongly depressing while IC connections were slightly facilitating (paired-pulse ratio was 0.68 $\pm$ 0.06 for TC and 1.19 $\pm$ 0.19 for IC, $p < 0.04$), and both pathways became strongly facilitating after partial blockade by the drug (paired-pulse ratio was 1.68 $\pm$ 0.33 for TC and 2.28 $\pm$ 0.36 for IC, controls versus MK-801, $p < 0.005$; Figure 9B). This change in the paired-pulse effect is consistent with each population of synapses having a range of p_r values (Huang and Stevens, 1997). MK-801 blocks synapses with highest p_r fastest, so that by the 100th stimulus the unblocked population becomes enriched in facilitating synapses with low p_r.

The blockade rates of single-shock EPSCs were significantly faster for the TC synapses than for the IC synapses (Figures 9C and 9D). The trend is also clear in the single-neuron results, where TC NMDA EPSCs were blocked faster than IC NMDA EPSCs in 9 of the 11 neurons. When data from all neurons under control ionic conditions were pooled, the average number of stimuli necessary to reach half amplitude was 27 $\pm$ 16 for the TC pathway and 41 $\pm$ 27 for the IC pathway ($p < 0.01$; Figure 9E). This pathway-specific difference in decay rates disappeared when MK-801 experiments were conducted in a medium containing 3 mM [Ca] and 1 mM [Mg]. Under these conditions, the average number of stimuli required to reach half amplitude was 11.1 $\pm$ 6.3 and 11.6 $\pm$ 4.6 for TC and IC synapses, respectively ($n = 4$), implying that high [Ca] both increased and normalized p_r in the two pathways. This result makes it unlikely that differences in the magnitude of the glutamate concentration transient in the clefts of the TC and IC synapses account for the different MK-801 decay rates. We conclude that the pathway-specific difference in the blockade rate of NMDA currents under normal ionic conditions was caused by the difference in the p_r of the two synapse types.

Estimating absolute values of p_r from the rate of MK-801 blockade requires a priori knowledge about the form of the distribution function of p_r in each population of synapses (Huang and Stevens, 1997), and we did not attempt to estimate these distributions. Regardless, our data clearly imply that the average p_r of TC synapses

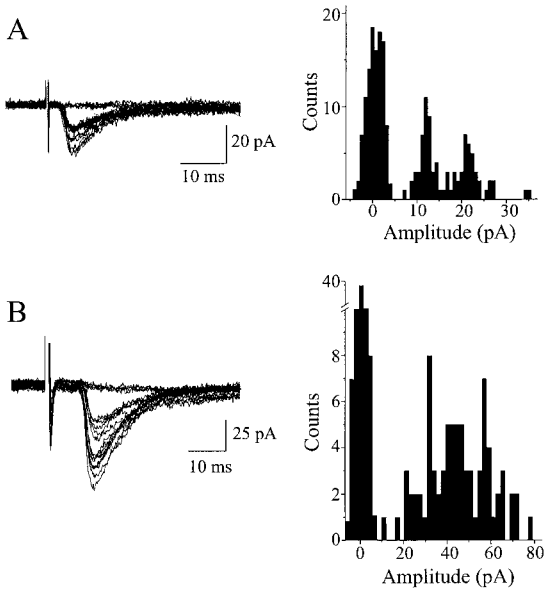

Figure 7. Efficacy of TC and IC Axons Using Minimal Stimulation under Control Conditions of [Ca] and [Mg]

(A) Recordings from a neuron showing all-or-none EPSCs in response to IC stimulation. Example traces shown on the left panel. The amplitude distribution histogram (right panel) shows two peaks at about 12 pA and 21 pA, suggesting two release sites.

(B) Data from another cell during typical minimal TC stimulation, showing larger and more variable amplitude responses than in most IC connections. Stimulus intensity in both cells was adjusted to give >60% failures.

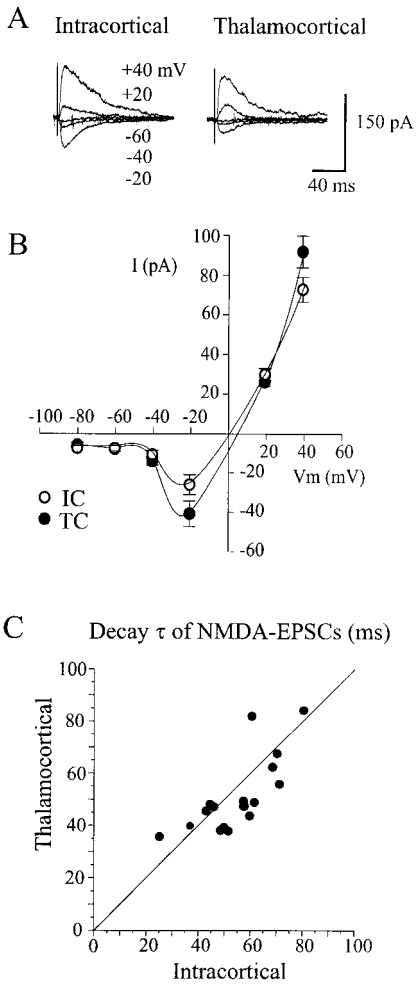

Figure 8. NMDA EPSCs from TC and IC Synapses Are Identical

(A) NMDA EPSCs were recorded with $GABA_A$ and AMPA receptors blocked. TC and IC responses were evoked at various holding potentials between −60 mV and +40 mV, as indicated.

(B) Voltage dependence of NMDA EPSCs from IC and TC synapses is indistinguishable. The graph shows pooled data from 20 neurons. Response amplitudes of TC and IC responses were adjusted to be similar at +20 mV by varying the stimulus intensity.

(C) Decay time constants of NMDA EPSCs varied widely across cells but were similar for TC and IC responses within cells. Each point represents data from one neuron (n = 17).

is higher than that of IC synapses. Since the MK-801 blockade rate is inversely proportional to p_r (Hessler et al., 1993; Rosenmund et al., 1993), then to a first approximation $p_{r(TC)}$ is on average about 1.5 times higher than $p_{r(IC)}$.

Discussion

Our results show that the efficacy of TC connections is substantially higher than that of IC connections within layer 4. There seem to be both anatomical and physiological reasons for this difference: (1) TC and IC synapses generate the same distributions of quantal size (q) and shape, but (2) the average TC axon contributes 3.2 times more release sites (n) than the average IC axon, and (3) the mean release probability (p_r) of TC synapses is roughly 1.5 times higher than that of IC synapses. Using the simple relation between efficacy and parameters of innervation, release probability, and quantal size, $E = q \cdot n \cdot p_r$, we can predict that each connection from a thalamic neuron to a layer 4 cortical neuron is, on average, about 4.8 times more effective than the connection between two cortical neurons. This provides a possible cellular mechanism for the observation, based on cross-correlation of spikes, that TC connections are about 10-fold more effective than IC connections in the cat visual system (Toyama et al., 1981; Tanaka, 1983; Reid and Alonso, 1996).

An alternative measure of single-axon efficacy could, in principle, be derived from minimal-stimulation experiments. Indeed, we found that the mean amplitude of TC responses under normal ionic conditions was about 2.6 times larger than that of IC responses. This ratio is close to the one reported by Stratford et al. (1996) for suspected TC connections and identified IC connections but smaller than the efficacy ratio we calculated in the preceding paragraph. At least one reason for this discrepancy is that there is no definitive way to distinguish failures of axonal activation from failures of transmitter release in minimal-stimulation experiments. Accordingly, the mean response amplitudes that we and Stratford et al. (1996) calculated were derived from successful events only; since p_r is higher in TC than in IC synapses, the ratios obtained from minimal stimulation underestimate the efficacy difference between TC and IC connections.

It is unlikely that synapse position, and resulting electrotonic differences, differentially distorted our measurements of TC and IC synapse properties. About 80% of the neurons in layer 4 of mouse cortex are small spiny stellate or pyramidal cells, and our stained cells were all small spiny types. Modeling suggests that these cells are electrotonically very compact (Segev et al., 1995). TC synapses constitute about 10%–20% of the excitatory synapses onto spiny layer 4 cells, but there is no evidence that TC and IC synapses are distributed differently along the dendrites (White and Keller, 1989). Finally, errors arising from electrotonic properties are more severe for voltage clamp than for current clamp measurements (Jack et al., 1994), yet our estimates of quantal sizes under both clamp modes gave identical results for TC and IC events.

We estimated that quantal size for both TC and IC synapses is about 11 pA at a membrane potential of −60 mV, yielding a peak quantal chord conductance of about 180 pS. In unclamped, Cs^+-filled neurons the quantal size was about 0.4 mV. Our results are similar to the quantal size of 10 pA (at −70 mV) estimated by Stern et al. (1992) for IC synapses in layer 4 nonpyramidal neurons of rat visual cortex, and they are in the same range as estimates made from other types of neocortical neurons and unidentified synapses (Hestrin, 1992; Volgushev et al., 1995; Buhl et al., 1997; Isaac et al., 1997; Turrigiano et al., 1998). Our amplitude estimates may have been slightly distorted by the methods we used. The EPSC kinetics we measured are slower than previously reported (e.g., Stern et al., 1992), probably due to filtering by our recording system. EPSPs in our experiments may have been boosted because Cs^+ blocked

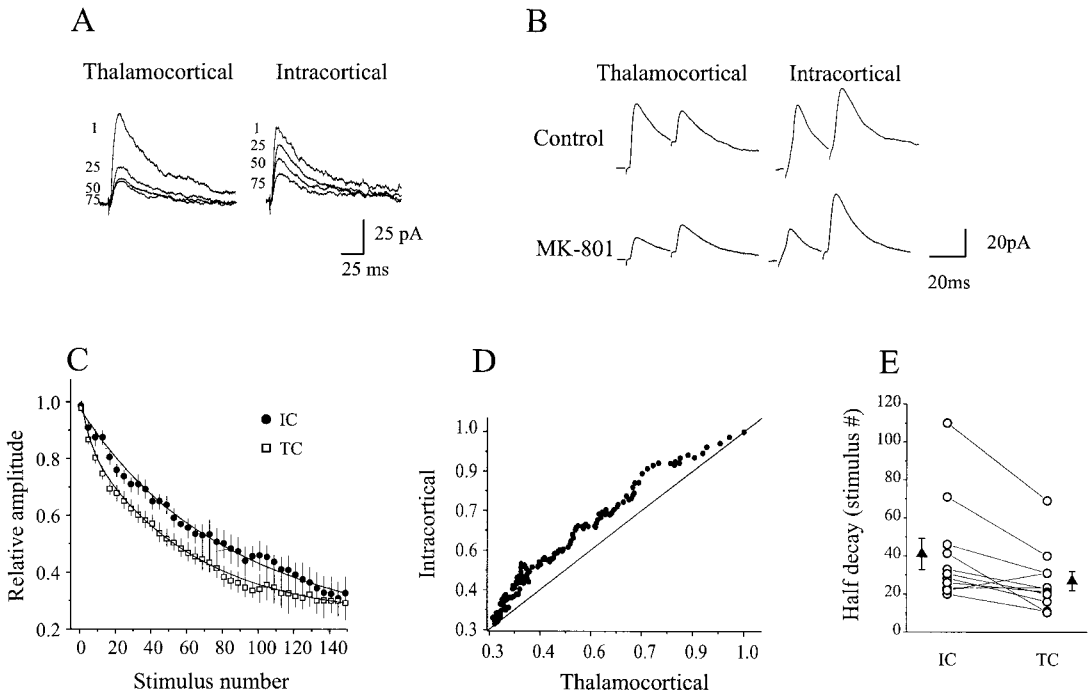

Figure 9. TC Synapses Have Higher Release Probability Than IC Synapses

(A) The amplitudes of NMDA receptor–dependent TC and IC EPSCs decrease gradually during repetitive stimulation in the presence of 40 μM MK-801. Shown are four traces each; stimulus sequence numbers are to the left. The holding potential was +40 mV.

(B) Paired-pulse stimuli elicited depression of NMDA receptor–dependent TC and IC EPSCs before the addition of MK-801 (upper traces), but responses showed facilitation by the time of the 100th stimulus in the presence of the drug (lower traces).

(C) Summary data showing progressive blockade of NMDA EPSCs by MK-801 in all cells tested (n = 11). TC EPSCs (open squares) decayed faster than IC EPSCs (closed circles). Data points and bars are mean ± SEM, and best-fit biexponential functions are superimposed.

(D) Same data as in (C), plotted as amplitudes of IC NMDA EPSCs against TC NMDA EPSCs. The response to the first stimulation of the two pathways is represented by the point at (1,1), and the reference line has a slope of 1.

(E) The MK-801-induced half-decay times, in terms of stimulus number, plotted for the TC and IC EPSCs of each of the 11 neurons tested. The corresponding values for individual cells (open circles) are connected with lines, and the mean ± SEM half-decay times for IC (left) and TC (right) are represented by closed triangles.

outward intrinsic currents. However, both distortions are likely to have affected the TC and IC pathways similarly. We can place high confidence in our conclusion that TC and IC quantal sizes are similar, since comparable results were obtained from several independent measures: evoked, pathway-specific responses in Sr^{2+} and in Cd^{2+}, spontaneous EPSCs in the same media, and the smallest minimal evoked responses in high [Ca]/[Mg] medium. The results suggest that all major types of excitatory synaptic release sites on layer 4 neurons, regardless of presynaptic source, contribute similar quantal size distributions.

Our results suggest that the average TC axon provides more release sites on a layer 4 neuron than do most IC axons. It is not possible to give full structural meaning to this conclusion. In some central systems, a release site seems to be anatomically equivalent to a synapse active zone (e.g., Korn et al., 1981; Walmsley, 1991; Gulyas et al., 1993; Schikorski and Stevens, 1997). Interestingly, about 90% of synapses in the neocortex have only one active zone each (Calverley and Jones, 1990; Peters and Harriman, 1990); single TC terminals in rat somatosensory cortex often have multiple active zones, while IC synapses do not (Kharazia and Weinberg, 1994). Our physiological estimate of the TC *n* (from 1 to 18, with a mean of about 7) suggests a wide range for the number of release sites between thalamic and layer 4 neurons. For *n* of IC connections, we estimated a range of 1–4, with a mean of 2.2. To our knowledge, no anatomical study has directly measured the number of synaptic contacts between a single thalamic relay cell and one cortical neuron, nor between neurons of layer 4. For comparison, very closely spaced, synaptically interconnected pyramidal cells in layer 5 make from 2 to 8 synaptic contacts (Deuchars et al., 1995; Markram et al., 1997).

There are several potential sources of bias in our estimates of *n*. First, because the slicing procedure removes some axonal branches, *n* for both pathways could be underestimated. Second, extracellular stimulation tends to select for larger diameter axons (Swadlow, 1998), which might have more release sites than thinner axons. This would probably influence measurements of IC axons most; while TC (ventral posterior medial nucleus of the thalamus or VPM) axons are myelinated and have a relatively low threshold for activation, most IC axons are unmyelinated, though some are larger and myelinated (Keller, 1995). Third, if p_r were different for IC and TC terminals, then our minimal-stimulation paradigm would tend to select for the pathway with the higher p_r. However, we used high [Ca]/[Mg] solutions both to increase

p_r and to equalize it between pathways. Fourth, because p_r is <1, even under conditions of high release, estimates of n for connections with the most release sites will be selectively underestimated. Assuming uniform and independent p_r, the probability of all sites releasing on a single trial (p_{all}) is simply $p_{all} = (p_r)^n$. We do not know the absolute values of p_r, although our one TC single-release site (Figures 4A–4C) suggested it was high ($p_r \approx 0.8$). More conservatively, if mean p_r is equal to 0.5 and n is equal to 7 (i.e., our estimate of n for the average TC axon), then p_{all} equals $\sim$0.008. In this case, our sample sizes would yield a reasonable estimate of n for many TC and IC axons but would underestimate n for the most highly connected TC axons. As p_r falls, the calculated n for most TC axons is increasingly underestimated; however, axons with small numbers of release sites remain well estimated. For example, if n is equal to 2 (i.e., our estimate for the average IC axon) and p_r is as low as 0.2, then p_{all} equals 0.04, giving us an excellent chance of measuring maximal potency. Thus, the difference in n between TC versus IC axons may actually be larger than our estimates imply.

TC synapses seem to have a higher average p_r than IC synapses in control solution, as suggested by their more prominent short-term depression (Gil et al., 1997) and, more definitively, by the results of our MK-801 experiments. The stronger short-term depression of TC synapses is likely to be the result of their higher p_r (cf. Debanne et al., 1996; Castro-Alamancos and Connors, 1997; Murthy et al., 1997). Both synapse populations may have widely varying p_r values, as suggested by the change in paired-pulse ratio during exposure to MK-801 (Figure 9B). For comparison, estimates of p_r for hippocampal synapses varied between 0.05 and 0.9 (Dobrunz and Stevens, 1997; Murthy et al., 1997). The structure of TC and IC synaptic terminals is consistent with our physiological data. In general, the volume of a presynaptic terminal correlates with the size and number of its active zones and docked vesicles and probably also correlates with its p_r (Korn and Faber, 1991; Pierce and Lewin, 1994; Schikorski and Stevens, 1997). Ultrastructural studies show that TC terminals are significantly larger than IC terminals in rat somatosensory cortex (Kharazia and Weinberg, 1994) and in the visual cortex (Ahmed et al., 1994). Unidentified synaptic events with characteristics similar to TC responses (unusually large size and strong depression) have been observed in neurons of the visual cortex of rats (Volgushev et al., 1995) and cats (Stratford et al., 1996), so our results may be generally applicable to sensory neocortex.

The efficacy of a cortical connection is not fixed. Both TC (Crair and Malenka, 1995; Isaac et al., 1997) and some IC connections (Bear and Malenka, 1994) express activity-dependent long-term potentiation and depression, and both pre- and postsynaptic mechanisms have been implicated. TC and IC synapses are also subject to short-term frequency-dependent changes in efficacy. In addition, we found that activating presynaptic $GABA_B$ receptors selectively depresses IC synapses, while the efficacy of TC synapses is selectively enhanced by activating presynaptic nicotinic acetylcholine receptors (Gil et al., 1997). These presynaptic effects also alter the short-term dynamics of the synapses and presumably are mediated by changes in p_r. The difference between $p_{r(TC)}$ and $p_{r(IC)}$ may be even larger in vivo, where ambient activation of GABAergic and cholinergic receptors is higher than in a slice.

The sparseness of TC boutons in layer 4 seems to imply that the connections from thalamus are relatively weak. But TC connections may be more reliable and potent than simple bouton numbers suggest, thanks perhaps to the high p_r and multiple release sites allowed by their large terminal size. The effectiveness of the TC pathway is also subject to other factors, such as the precise alignment of thalamic axons and cortical targets (Reid and Alonso, 1995; Ferster et al., 1996), the control of feedforward inhibition in the cortex (Simons and Carvell, 1989; Agmon and Connors, 1992; Simons, 1995; Swadlow, 1995; Gil and Amitai, 1996), and the recruitment of recurrent IC excitatory circuits (Kyriazi and Simons, 1993; Douglas et al., 1995; Castro-Alamancos and Connors, 1996). There is strong evidence that patterns of TC connections are a primary determinant of some receptive field properties of neurons in visual cortex (Hubel and Wiesel, 1962; Ferster et al., 1996; Reid and Alonso, 1996). The relatively high efficacy of TC connections may be one of the reasons that aligned axons from the lateral geniculate nucleus can strongly drive cortical neurons in layer 4 in an orientation-selective manner. The relative strength of TC connections compared to IC connections is likely to be a key factor in other forms of cortical processing as well.

Experimental Procedures

Preparation

TC slices, 450 μm thick, were prepared as described previously (Agmon and Connors, 1991; Gil and Amitai, 1996). Briefly, 2- to 3-week-old albino mice (CD/1) were anesthetized with pentobarbital sodium and decapitated, and their brains were quickly immersed in ice-cold oxygenated artificial cerebrospinal fluid (ACSF) composed of (in mM): 124 NaCl, 3 KCl, 2 $MgSO_4$, 1.25 $NaHPO_4$, 2 $CaCl_2$, 26 $NaHCO_3$, and 10 dextrose, saturated with 95% O_2/5% CO_2 (pH 7.4, 310 mOsm). TC slices were cut on a vibratome (Campden Instruments) and placed in a holding chamber that contained ACSF at room temperature for at least 1 hr. The recording chamber maintained the slices at the fluid–gas interface at a temperature of 27°C–28°C.

Stimulation, Recording, and Drugs

Whole-cell recordings were made from layer 4 neurons in the barrel field. Patch recording micropipettes (4 MΩ) were filled with a solution containing (in mM) 125 Cs gluconate, 2 $MgCl_2$, 6 CsCl, 10 HEPES and 1 QX-314 (pH 7.2, 280 mOsm). Voltages or currents were recorded with a patch clamp amplifier (Axon Instruments), low-pass filtered at 2–5 kHz, and digitally sampled at 5–10 kHz. Series resistance was typically $<$15 MΩ. In general, resting potential was held at $-$60 mV under voltage clamp. Cs^+-filled electrodes were used in current clamp experiments in order to improve the visibility of small postsynaptic events, and in these cases resting potential was maintained by injecting small, steady hyperpolarizing currents. One bipolar stimulating electrode was placed in layer 4 at least 0.5 mm medial to the recording area, to activate local horizontal IC fibers, while minimizing the activation of ascending TC fibers. The other stimulating electrode was placed in the ventrobasal nucleus of the thalamus. The two pathways were stimulated alternately, typically every 5 s (0.1 Hz for each pathway), using pulses of 100–200 μs and about 50 μA.

Recordings were made from neurons in the region that generated the largest field potential response to thalamic stimulation, and EPSPs or EPSCs were judged to be monosynaptic using criteria of short latency and stable, monophasic time course (for details, see

Gil and Amitai, 1996; Gil et al., 1997). Crossed paired pulses were used to verify that stimuli of one tract were not contaminated by activation of axons from the other tract (Gil et al., 1997). In some experiments, biocytin (0.1%) was included in the pipette solution, and the slices were processed by standard avidin-biotin-peroxidase procedures (Horikawa and Armstrong, 1988).

The transmitter receptor blockers bicuculline methiodide (BMI, 5 μM; RBI), D,L-2-amino-5-phosphonovalerate (APV, 30 μM; RBI), 6,7-dinitroquinoxaline-2,3-dione (DNQX, 15 μM; RBI), and MK-801 (40 μM) were added to the perfusate. In some experiments, Ca^{2+} was replaced by 4 mM [Sr] and [Mg] was raised to 4 mM, and the solution was introduced at least 15 min before recording started.

Minimal Stimulation

During minimal-stimulation experiments, we used a bathing solution containing 3 mM [Ca] and 1 mM [Mg]. To apply as focal a stimulus as possible, we developed a homemade stimulating electrode from 2 mm outside diameter glass tubing with a θ cross section. The glass was pulled in a conventional two-stage puller to a tip size of $<$10 μm in diameter. Each side of the tubing was filled with ACSF, and electrical contact was made through two AgCl wires pushed as close as possible to the tip. The tip was gently pushed into the slice, and low stimulus intensities ($<$10 μA, 0.1–0.2 ms duration) were used to minimize the area of activation; such stimuli always failed to evoke a measurable field potential near the recorded cortical neuron. The criteria for single-axon stimulation were: (1) all-or-none synaptic events, (2) little or no variation in EPSC latencies, (3) a small change in the stimulus intensity did not change the mean size or shape of the EPSC, and (4) lowering stimulus intensities by 10%–20% resulted in complete failure to evoke EPSCs. Typically, 150–200 trials were obtained from each cell.

Data Analysis

Unitary EPSPs or EPSCs and spontaneous events were detected by threshold and by the first derivative (Malgaroli and Tsien, 1992; Oliet et al., 1996) and were inspected by eye with software programmed under the LabView environment (National Instruments). Baseline noise was measured during a 5 ms time window preceding each measured event. The signal-to-noise ratio for quantal EPSCs was calculated as the ratio between the mean event amplitude and the standard deviation of the noise, and was very similar for both tracts (9.2 for the TC tract and 9.4 for the IC tract). Thus, there is no reason to suspect that we have missed a substantial number of events in either pathway or that events were differentially missed. The progressive block of NMDA EPSCs in the presence of MK-801 was fitted with a biexponential curve, using a simplex fitting algorithm to minimize χ^2 (Kullmann et al., 1996). For analysis of EPSC/P amplitude distributions, a sum of Gaussian functions was fitted to the histograms by the method of least squares (Paulsen and Heggelund, 1994). Statistical comparisons were made with the Wilcoxon test for paired samples, the Mann-Whitney test for unpaired samples, or t tests. The coefficient of variation (CV) was defined as $(\sigma_s^2 - \sigma_n^2)^{1/2}/\mu_s$, where σ_s and σ_n are the variances of the synaptic measurements and noise, respectively, and μ_s is the mean synaptic size. The comparison between the TC and the IC cumulative distributions was made using the resampling (bootstrapping) method (Van der Kloot, 1996). Unless specified, data are reported as mean ± SD.

Acknowledgments

We thank Michael Beierlein, Gerald Finnerty, Jay Gibson, Carole Landisman, David Pinto, and Clay Reid for comments on the manuscript. This work was supported by a grant from the Israel Science Foundation (Y. A.), a Fogarty International Collaboration Research Award (TW00743 from NIH) (Y. A. and B. W. C.), and grant NS25983 (NIH) (B. W. C.). Z. G. is a Fellow of the Kreitman School of Advanced Studies.

Received December 16, 1998; revised April 28, 1999.

References

Abdul-Ghani, M.A., Valiante, T.A., and Pennefather, P.S. (1996). Sr^{2+} and quantal events at excitatory synapses between mouse hippocampal neurons in culture. J. Physiol. (Lond.) *495*, 113–125.

Agmon, A., and Connors, B.W. (1991). Thalamocortical responses of mouse somatosensory (barrel) cortex in vitro. Neuroscience *41*, 365–379.

Agmon, A., and Connors, B.W. (1992). Correlation between intrinsic firing patterns and thalamocortical synaptic responses of neurons in mouse barrel cortex. J. Neurosci. *12*, 319–329.

Ahmed, B., Anderson, J.C., Douglas, R.J., Martin, K.A.C., and Nelson, J.C. (1994). Polyneuronal innervation of spiny stellate neurons in cat visual cortex. J. Comp. Neurol. *341*, 39–49.

Bear, M.F., and Malenka, R.C. (1994). Synaptic plasticity: LTP and LTD. Curr. Opin. Neurobiol. *4*, 389–399.

Buhl, E.H., Tamas, G., Szilagyi, T., Stricker, C., Paulsen, O., and Somogyi, P. (1997). Effect, number and location of synapses made by single pyramidal cells onto aspiny interneurones of cat visual cortex. J. Physiol. (Lond.) *500*, 689–713.

Calverley, R.K.S., and Jones, D.G. (1990). Contribution of dendritic spines and perforated synapses to synaptic plasticity. Brain Res. Rev. *15*, 215–249.

Castro-Alamancos, M.A., and Connors, B.W. (1996). Short-term plasticity of a thalamocortical pathway dynamically modulated by behavioral state. Science *272*, 274–277.

Castro-Alamancos, M.A., and Connors, B.W. (1997). Distinct forms of short-term plasticity at excitatory synapses of hippocampus and neocortex. Proc. Natl. Acad. Sci. USA *94*, 4161–4166.

Chance, F.S., Nelson, S.B., and Abbott, L.F. (1998). Synaptic depression and temporal response characteristics of V1 cells. J. Neurosci. *18*, 4785–4799.

Chung, S., and Ferster, D. (1998). Strength and orientation tuning of the thalamic input to simple cells revealed by electrically evoked cortical suppression. Neuron *20*, 1177–1189.

Crair, M.C., and Malenka, R.C. (1995). A critical period for long-term potentiation at thalamocortical synapses. Nature *375*, 325–328.

Debanne, D., Guerineau, N.C., Gahwiler, B.H., and Thompson, S.M. (1996). Paired-pulse facilitation and depression at unitary synapses in rat hippocampus: quantal fluctuation affects subsequent release. J. Physiol. (Lond.) *491*, 163–175.

Deuchars, J., West, D.C., and Thomson, A.M. (1995). Relationships between morphology and physiology of pyramid–pyramid single axon connections in rat neocortex in vitro. J. Physiol. (Lond.) *478*, 423–435.

Dobrunz, L.E., and Stevens, C.F. (1997). Heterogeneity of release probability, facilitation, and depletion at central synapses. Neuron *18*, 995–1008.

Dodge, F.A., Miledi, R., and Rahamimoff, R. (1969). Sr^{2+} and quantal release of transmitter at the neuromuscular junction. J. Physiol. *200*, 267–284.

Douglas, R.J., Koch, C., Mahowald, M., Martin, K.A.C., and Suarez, H.H. (1995). Recurrent excitation in neocortical circuits. Science *269*, 981–985.

Ferster, D., Chung, S., and Wheat, H. (1996). Orientation selectivity of thalamic input to simple cells of cat visual cortex. Nature *380*, 249–252.

Fleidervish, I.A., Binshtok, A.M., and Gutnick, M.J. (1998). Functionally distinct NMDA receptors mediate horizontal connectivity within layer 4 of mouse barrel cortex. Neuron *21*, 1055–1065.

Gil, Z., and Amitai, Y. (1996). Properties of convergent thalamocortical and intracortical synaptic potentials in single neurons of neocortex. J. Neurosci. *16*, 6567–6578.

Gil, Z., Connors, B.W., and Amitai, Y. (1997). Differential modulation of neocortical synapses by neuromodulators and activity. Neuron *19*, 679–686.

Gulyas, A.I., Miles, R., Sik, A., Toth, K., Tamamaki, N., and Freund, T.F. (1993). Hippocampal pyramidal cells excite inhibitory neurons through a single release site. Nature *366*, 683–687.

Hessler, N.A., Shirke, A.M., and Malinow, R. (1993). The probability of transmitter release at a mammalian central synapse. Nature *366*, 569–572.

Hestrin, S. (1992). Activation and desensitization of glutamate–activated channels mediating fast excitatory synaptic currents in the visual cortex. Neuron *9*, 991–999.

Horikawa, K., and Armstrong, W.E. (1988). A versatile means of intracellular labeling: injection of biocytin and its detection with Avidin conjugates. J. Neurosci. Methods *25*, 1–11.

Huang, E.P., and Stevens, C.F. (1997). Estimating the distribution of synaptic reliabilities. J. Neurophysiol. *78*, 2870–2880.

Hubel, D.H., and Wiesel, T.N. (1962). Receptive fields, binocular interaction and functional architecture in the cat's visual cortex. J. Physiol. (Lond.) *160*, 106–154.

Isaac, J.T., Crair, M.C., Nicoll, R.A., and Malenka, R.C. (1997). Silent synapses during development of thalamocortical inputs. Neuron *18*, 269–280.

Jack, J.J.B., Larkman, A.U., Major, G., and Stratford, K.J. (1994). Quantal analysis of the synaptic excitation of CA1 hippocampal pyramidal cells. In Molecular and Cellular Mechanisms of Neurotransmitter Release, L. Stjarne, P. Greengard, S. Grillner, T. Hokfelt, and D. Ottoson, eds. (New York: Raven Press), pp. 275–299.

Johnson, M.J., and Alloway, K.D. (1996). Cross-correlation analysis reveals laminar differences in thalamocortical interactions in the somatosensory system. J. Neurophysiol. *75*, 1444–1457.

Katz, B. (1969). The Release of Neural Transmitter Substance (Liverpool, UK: University Press).

Keller, A. (1995). Synaptic organization of the barrel cortex. In Cerebral Cortex, Volume 11: The Barrel Cortex of Rodents, E.G. Jones and I.T. Diamond, eds. (New York: Plenum Press), pp. 221–262.

Kharazia, V.N., and Weinberg, R.J. (1994). Glutamate in thalamic fibers terminating in layer IV of primary sensory cortex. J. Neurosci. *14*, 6021–6032.

Korn, H., and Faber, D.S. (1991). Quantal analysis and synaptic efficacy in the CNS. Trends Neurosci. *14*, 439–445.

Korn, H., Triller, A., Mallet, A., and Faber, D.S. (1981). Fluctuating responses at a central synapse: n of binomial fit predicts number of stained presynaptic boutons. Science *213*, 898-901.

Kullmann, D.M., Erdemli, G., and Asztely, F. (1996). LTP of AMPA and NMDA receptor–mediated signals: evidence for presynaptic expression and extrasynaptic glutamate spill-over. Neuron *17*, 461–474.

Kyriazi, H.T., and Simons, D.J. (1993). Thalamocortical response transformation in simulated whisker barrels. J. Neurosci. *13*, 1601–1615.

Malgaroli, A., and Tsien, R.W. (1992). Glutamate-induced long–term potentiation of the frequency of miniature synaptic currents in cultured hippocampal neurons. Nature *357*, 134–139.

Manabe, T., and Nicoll, R.A. (1994). Long-term potentiation: evidence against an increase in transmitter release probability in the CA1 region of the hippocampus. Science *265*, 1888–1892.

Markram, H., Lubke, J., Frotscher, M., and Sakmann, B. (1997). Physiology and anatomy of synaptic connections between thick tufted pyramidal neurons in the developing rat neocortex. J. Physiol. (Lond.) *500*, 409–440.

Mason, A., Nicoll, A., and Stratford, K. (1991). Synaptic transmission between individual pyramidal neurons of the rat visual cortex in vitro. J. Neurosci. *11*, 72–84.

McGuire, B.A., Hornung, J.-P., Gilbert, C.D., and Weisel, T.N. (1984). Patterns of synaptic input to layer 4 of cat striate cortex. J. Neurosci. *4*, 3021–3033.

Murthy, V.N., Sejnowski, T.J., and Stevens, C.F. (1997). Heterogeneous release properties of visualized individual hippocampal synapses. Neuron *18*, 599–612.

Oliet, S.H.R., Malenka, R.C., and Nicoll, R.A. (1996). Bidirectional control of quantal size by synaptic activity in the hippocampus. Science *271*, 1294–1297.

Paulsen, O., and Heggelund, P. (1994). The quantal size at retinogeniculate synapses determined from spontaneous and evoked EPSCs in guinea-pig thalamic slices. J. Physiol. (Lond.) *480*, 505–511.

Peters, A., and Harriman, K.M. (1990). Different kinds of axon terminals forming symmetric synapses with the cell bodies and initial axon segments of layer II/III pyramidal cells. I. Morphometric analysis. J. Neurocytol. *19*, 154–174.

Peters, A., and Payne, B.R. (1993). Numerical relationships between geniculocortical afferents and pyramidal cell modules in cat primary visual cortex. Cereb. Cortex *3*, 69–78.

Pierce, J.P., and Lewin, G.R. (1994). An ultrastructural size principle. Neuroscience *58*, 441–446.

Raastad, M., Storm, J.F., and Andersen, P. (1992). Putative single quantum and single fiber excitatory postsynaptic currents show similar amplitude range and variability in rat hippocampal slices. Eur. J. Neurosci. *4*, 113–117.

Reid, R.C., and Alonso, J.-M. (1995). Specificity of monosynaptic connections from thalamus to visual cortex. Nature *378*, 281–284.

Reid, R.C., and Alonso, J.-M. (1996). The processing and encoding of information in the visual system. Curr. Opin. Neurobiol. *6*, 475–480.

Reid, C.A., Clements, J.D., and Bekkers, J.M. (1997). Nonuniform distribution of Ca^{2+} channel subtypes on presynaptic terminals of excitatory synapses in hippocampal cultures. J. Neurosci. *17*, 2738–2745.

Rosenmund, C., Clements, J.D., and Westbrook, G.L. (1993). Nonuniform probability of glutamate release at a hippocampal synapse. Science *262*, 754–757.

Schikorski, T., and Stevens, C.F. (1997). Quantitative ultrastructural analysis of hippocampal excitatory synapses. J. Neurosci. *17*, 5858–5867.

Segev, I., Friedman, A., White, E.L., and Gutnick, M.J. (1995). Electrical consequences of spine dimensions in a model of a cortical spiny stellate cell completely reconstructed from serial thin sections. J. Comput. Neurosci. *2*, 117–130.

Simons, D.J. (1995). Neuronal integration in the somatosensory whisker/barrel cortex. In Cerebral Cortex, Volume 11: The Barrel Cortex of Rodents, E.G. Jones and I.T. Diamond, eds. (New York: Plenum Press), pp. 263–297.

Simons, D.J., and Carvell, G.E. (1989). Thalamocortical response transformation in the rat vibrissa/barrel system. J. Neurophysiol. *61*, 311–330.

Somers, D.C., Nelson, S.B., and Sur, M. (1995). An emergent model of orientation selectivity in cat visual cortical simple cells. J. Neurosci. *15*, 6700–6719.

Stern, P., Edwards, F.A., and Sakmann, B. (1992). Fast and slow components of unitary EPSCs on stellate cells elicited by focal stimulation in slices of rat visual cortex. J. Physiol. (Lond.) *449*, 247–278.

Stevens, C.F., and Wang, Y. (1995). Facilitation and depression at single central synapses. Neuron *14*, 795–802.

Stratford, K.J., Tarczy-Hornoch, K., Martin, K.A.C., Bannister, N.J., and Jack, J.J.B. (1996). Excitatory synaptic inputs to spiny stellate cells in cat visual cortex. Nature *382*, 258–261.

Swadlow, H.A. (1995). Influence of VPM afferents on putative inhibitory interneurons in S1 of the awake rabbit: evidence from cross-correlation, microstimulation, and latencies to peripheral sensory stimulation. J. Neurophysiol. *73*, 1584–1599.

Swadlow, H.A. (1998). Neocortical efferent neurons with very slowly conducting axons: strategies for reliable antidromic identification. J. Neurosci. Methods *79*, 131–141.

Tanaka, K. (1983). Cross-correlation analysis of geniculostriate neuronal relationships in cats. J. Neurophysiol. *49*, 1303–1318.

Thomson, A.M., Deuchars, J., and West, D.C. (1993). Single axon excitatory postsynaptic potentials in neocortical interneurons exhibit pronounced paired pulse facilitation. Neuroscience *54*, 347–360.

Toyama, K., Kimura, M., and Tanaka, K. (1981). Cross-correlation analysis of interneuronal connectivity in cat visual cortex. J. Neurophysiol. *46*, 191–201.

Turrigiano, G.G., Leslie, K.R., Desai, N.S., Rutherford, L.C., and Nelson, S.B. (1998). Activity-dependent scaling of quantal amplitude in neocortical neurons. Nature *391*, 892–895.

Van der Kloot, W. (1996). Statistics for studying quanta at synapses: resampling and confidence limits on histograms. J. Neurosci. Methods *65*, 151–155.

Volgushev, M., Voronin, L.L., Chistiakova, M., Artola, A., and Singer, W. (1995). All-or-none excitatory postsynaptic potentials in the rat visual cortex. Eur. J. Neurosci. *7*, 1751–1760.

Walmsley, B. (1991). Central synaptic transmission: studies at the connection between primary afferent fibers and dorsal spinocerebellar tract (DSCT) neurons in Clarke's column of the spinal cord. Prog. Neurobiol. *36*, 391–423.

Walmsley, B., Alvarez, F.J., and Fyffe, R.E. (1998). Diversity of structure and function at mammalian central synapses. Trends Neurosci *21*, 81–88.

White, E.L., and Keller, A. (1989). Cortical Circuits: Synaptic Organization of the Cerebral Cortex—Structure, Function and Theory (Boston: Birkhauser).

Zucker, R.S. (1989). Short-term synaptic plasticity. Annu. Rev. Neurosci. *12*, 13–31.